Journal of
Nanoscience and Nanotechnology
Vol. 10, 1–7, 2010

High Frequency Electromechanical Memory Cells Based on Telescoping Carbon Nanotubes

A. M. Popov[1], Y. E. Lozovik[1], A. S. Kulish[2], and E. Bichoutskaia[3,*]

[1] *Institute of Spectroscopy, Russian Academy of Science, Fizicheskaia Street, Troitsk, Moscow Region 142190, Russia*
[2] *Moscow Institute of Steel and Alloys, Leninskii prosp. 4, Moscow 117936, Russia*
[3] *Department of Chemistry, University of Nottingham, University Park, Nottingham, NG7 2RD, United Kingdom*

A new method to increase the operational frequency of electromechanical memory cells based on the telescoping motion of multi-walled carbon nanotubes through the selection of the form of the switching voltage pulse is proposed. The relative motion of the walls of carbon nanotubes can be controlled through the shape of the interwall interaction energy surface. This allows the use of the memory cells in nonvolatile or volatile regime, depending on the structure of carbon nanotube. Simulations based on *ab initio* and semi-empirical calculations of the interwall interaction energies are used to estimate the switching voltage and the operational frequency of volatile cells with the electrodes made of carbon nanotubes. The lifetime of nonvolatile memory cells is also predicted.

Keywords:

RESEARCH ARTICLE

1. INTRODUCTION

Throughout the past decade, the unique mechanical and electrical properties of carbon nanotubes have been routinely exploited in nanoelectromechanical systems (NEMS). A variety of nanoscale electromechanical switches,[1–6] mainly based on bending of cantilever carbon nanotubes towards the substrate, have been fabricated whose switching behaviour depends on the nanotube length and is controlled through the balance between electrostatic, elastostatic and Van der Waals forces. The ability of the switches to hold both 0 (OFF) and 1 (ON) the logical states opens up further possibilities for using them in memory devices. The achievement of the controlled and reversible telescopic extension of multi-walled carbon nanotubes (MWNTs)[7–9] led to a new design of an electromechanical switch based on carbon nanotubes,[10] and the first memory cell based on low-friction bearing of carbon nanotubes had been fabricated soon after.[11]

The essential characteristic of the system operating as an electromechanical memory cell is so called bi-stability, or in other words the existence of two minima in the potential energy profile of the device. Figure 1 shows how these two minima can be used as a nonconducting the logical state 0 and a conducting the logical state 1 of a three-terminal memory cell based on a telescoping double-walled carbon nanotube (DWNT). For the memory cell shown in the Figure 1, the switching between the states 0 and 1 is realized by applying a voltage to a gate electrode. The designs without a gate electrode have been previously suggested for memory cells based on both cantilever nanotubes[12, 13] and telescopic extension of nanotubes.[14–16] Further details on the operational principles of a variety of nanotube-based electromechanical memory cells can be found in review.[17] A nonvolatile memory device can retain the state 1, and hence store information even when not powered. Nonvolatile memory is typically used as a secondary long-term continuing storage. A volatile form of memory, typically used for primary data storage, is random access memory. When computer is shut down, all the information contained in volatile memory is lost.

In recent experiments,[1–6, 11] a variety of electromechanical memory cells based on carbon nanotubes has been realized, and a wide range of their static characteristics investigated. However, the study of the dynamic properties and behaviour of these devices largely remains in the expanding domain of theoretical and computational modelling. The modelling shows that in nanotube-based electromechanical memory cells a carbon nanotube, which moves in response to applied voltage, undergoes significant oscillations after the switch between the the logical states.[16, 18–20] These oscillations do not affect unambiguous determination of a nonconducting state 0, and hence do not contribute to the switching time to this state. The switching time to the state 0 was theoretically estimated as being less than 1 ps for memory cells based on telescoping

*Author to whom correspondence should be addressed.

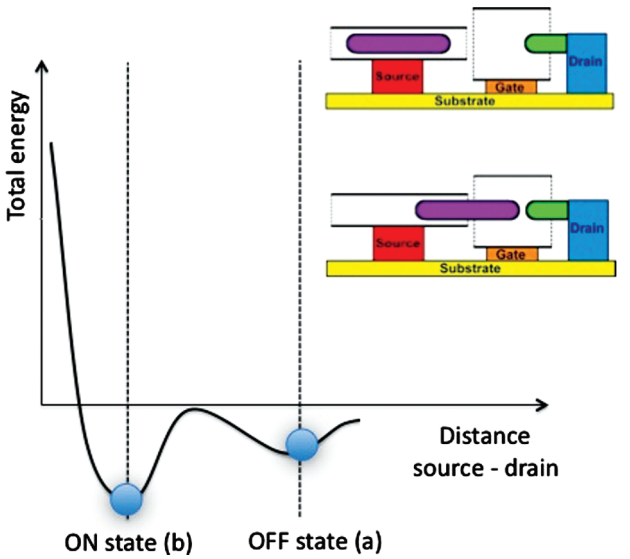

Fig. 1. Schematic representation of a three-terminal electromechanical memory cell based on telescoping DWNT in state 0 (a) and state 1 (b) and corresponding potential energy profile of the device.

nanotubes[16] and about 20 ps for memory cells based on cantilever nanotubes.[18] However, after the switching to the conducting state 1, the damping oscillations of the nanotube imply temporary but continuous change in the distance between the electrodes. Since the tunneling current between the electrodes depends exponentially on the distance between them, the nanotube oscillations lead to considerable variations in the current.[16, 18, 20] As a result, the determination of the state 1 is only possible after the oscillations of the nanotube (a movable element in the memory cell) completely vanish. This effect is not important in nonvolatile memory cells, since in such devices the information does not need to be read out immediately after it was written into the device. However, in volatile cells these oscillations represent the principal effect restricting the operational frequency. The oscillations increase the switching time up to 800 ps for memory cells based on cantilever nanotubes,[18] up to 100 ps for memory cells based on telescoping nanotubes,[16] up to 10–40 ns for the cells based on suspended nanotubes,[20] and up to 1 ns for two-terminal memory cells based on DWNTs with a short inner wall incapsulated inside a long outer wall.[19] In nanotube-based NEMS, high values of the quality factor (Q-factor) have also been reported. For oscillators based on the relative vibrations of the walls of a DWNT, Q-factor lies in the range of 10 to 1000 (see Ref. [21] and therein), for resonators based on suspended nanotubes $Q = 40 - 1000$ (Refs. [22–24]), and for resonators based on cantilever nanotubes $Q = 150 - 2500$ (Refs. [25–28]). If the oscillations are restricted by the presence of second electrode the value of Q-factor is only twice smaller.[29]

In present work, we propose and test in computational simulations a new method to increase the operational frequency of a nanoelectromechanical volatile cell. The oscillations of a moving element after switching to the the logical state 1 can be precluded if the moving element arrives to the position corresponding to the state 1 with zero kinetic energy. In order to achieve this, we propose the use of a variable form of the switching voltage pulse which governs the following three major stages. At first, a voltage pulse is applied to transfer kinetic energy to the movable element of a memory cell, then the motion of the element with decreasing velocity is established which is governed by the action of elastostatic and/or van der Waals forces between the components of the cell, and, finally, the holding voltage is applied at the moment in time when the moving element has reached zero velocity. The holding voltage is defined as the voltage necessary to hold a volatile cell in the state 1.

The dynamic behaviour of nanoelectromechanical memory cells based on suspended and cantilever nanotubes have been studied extensively theoretically.[12, 13, 18, 20, 30–33] However, novel designs of memory cells based on telescoping carbon nanotubes[14–16] have not yet received much deserved attention. One of the designs shown in Figure 1 is an all carbon three-terminal memory cell which comprises a single-walled carbon nanotube attached to the drain electrode, a telescoping carbon nanotube attached to the source electrode, and a large-diameter carbon nanotube attached to the gate electrode in which the core of inner walls was removed using a nanomanipulator (the technique for removal of the core from MWNTs has been proposed in Ref. [8]). The conditions allowing the use of this memory cell in nonvolatile or volatile storage have been described in Ref. [15]. The design has the following major advantages: a smaller size of nanotube-made drain and gate electrodes, compared to metal electrodes, can be realized; a smaller interaction force between the electrodes allows constructing an easy-to-operate all carbon volatile cell; good uniformity can be achieved using identical memory cells made of nanotubes with the same chirality indices.

It is worth noting that an all carbon memory cell based on telescoping nanotubes without the gate electrode has been already produced experimentally,[11] and a considerable further progress has been achieved in nanotechnology techniques in the field of NEMS production. A nanomanipulator can be now attached to a MWNT in order to move individual walls,[8, 9] manipulation with SWNTs is routinely possible,[34] the caps can be removed from carbon nanotubes,[35, 36] nanotubes can be cut into pieces of desirable length.[37] Recently, the techniques for unambiguous determination of chirality indices of both walls of DWNTs[38] have been successfully demonstrated. A variety of methods for preferential synthesis and separation of SWNTs with a given chirality index has been elaborated,[39] which could be used in fabrication of memory cells with identical structural characteristics. This gives us a cause for optimism that all carbon three-terminal memory cells

based on telescoping carbon nanotubes will be fabricated in the near future.

All carbon three-terminal memory cells based on telescoping nanotubes were therefore chosen to test the proposed form of the switching voltage pulse and to study the operational characteristics. It has been shown that in the volatile memory cells the mechanical oscillations can be completely damped after the switching to the the logical state 1 thus achieving the operational frequency of as high as 100 GHz. The dependencies on the cell size of the switching voltage between the states 0 and 1 have been calculated. The nonvolatile regime has also been studied, and the lifetime in the state 1 has been predicted for the nonvolatile cells.

2. COMPUTATIONAL DETAILS AND DISCUSSION OF RESULTS

The study of the balance of forces determining the operation of the nanoelectromechanical memory cell based on telescopic motion of the walls of carbon nanotubes requires the computation of the interaction energy between the walls and the barriers to their relative sliding. For a (5,5)@(10,10 DWNT, these values are calculated using the density functional theory (DFT) AIMPRO supercell code within the local density approximation.[40] Within the AIMPRO code, the pseudowave functions are described by 4 atom-centered Gaussian functions per atom expanded in spherical harmonics up to $l = 1$, with the second smallest exponent expanded to $l = 2$. The unit cell consists of 60 carbon atoms. The Brillouin zone sampling has been performed using 18 special k-points in the direction of the nanotube axis. Nonlocal, norm-conserving pseudopotential[41] and the Perdew-Wang exchange-correlation functional[42] have been used. Minima in the total energy were found using a conjugate gradient scheme. Positions of the atoms in the isolated (5,5) and (10,10) walls have been optimized. The interwall interaction energy U_{int} was calculated as the difference between the total energies of the optimized structures of (5,5)@(10,10) DWNT and separate (5,5) and (10,10) single-walled carbon nanotubes (SWNTs).

The telescopic extension of a DNWT attached to the source electrode (see Fig. 1) by pulling the inner wall out gives rise to the capillary force F_c which pushes the wall back inside the outer wall. If the distance between the edges of the fixed and moving walls is greater than 1 nm, the edge effects can be disregarded and the capillary force can be considered independent on the overlap between the walls. Thus, the average value of F_c can be derived as $F_c = U_{\text{int}}/l_{\text{uc}}$, where l_{uc} is the length of the unit cell of a DWNT. In the case of the (5,5)@(10,10) DWNT, the interwall interaction energy U_{int} was found to be 0.953 eV per unit cell, and the capillary force F_c is estimated as 0.625 nN. The structures of the nanotube caps have been obtained using the Q-Chem quantum chemistry package.[43] The Lennard-Jones potential $U = 4\epsilon((\sigma/r)^{12} - (\sigma/r)^6)$ was used to calculate the interaction between the nanotube caps considered to be the electrodes of the memory cell. Parameters[44] $\sigma = 3.44$ Å, $\epsilon = 2.62 \cdot 10^{-3}$ eV have been used for the interaction between carbon atoms.

The operation of the memory cell shown in Figure 1 is determined by the balance of forces applied to the moving inner wall of the DWNT attached to the source electrode. These forces are the attraction force, F_a, of the Van der Waals interaction between the source and drain electrodes, the electrostatic force, F_e, between the source electrode and drain or/and gate electrodes, as well as the forces of the interaction between the inner and outer walls of the source electrode. The latter comprise the capillary force, F_c, which retracts the inner wall back into the outer wall during the telescopic motion, and the static friction force, F_f, which arises due to the lateral interaction of the walls. The the logical state 0 of the memory cell is established when the inner wall of the DWNT is retracted into the outer wall (Fig. 1(a)). The state 1 corresponds to the position at which the inner wall is attracted to the drain electrode by the Van der Waals or/and the electrostatic forces (Fig. 1(b)).

In the absence of applied voltage, the condition for bistability of the memory cell is defined as $F_f + F_a > F_c$. If this condition is satisfied the memory cell can be used in nonvolatile regime. The static friction force F_f is determined by the structure of the walls moving relative to each other. According to DFT[45] and semiempirical[46] calculations, the friction force $F_f \approx 0$ for DWNTs with incommensurate or/and chiral walls. Experiments also show that the friction force is below the accuracy of measurements having the value of $1.4 \cdot 10^{-15}$ N/atom.[9] Thus, for the memory cells based on telescoping nanotubes with incommensurate or chiral walls, condition for bistability of the cell is further simplified leading to the following expression $F_a > F_c$. The balance of forces in the memory cells based on telescoping nanotubes having drain electrode made of different materials has been studied previously.[15] It was shown that if the friction force is negligible, a memory cell with both electrodes made of carbon nanotubes is stable in the state 1 only if the voltage is applied. Therefore such cell could be used as an easy-to-operate volatile cell.

The stability of the nonvolatile all carbon memory cell is studied based on the cell with the source electrode taken to be a (5,5)@(10,10) DWNT and the drain electrode taken to be a (5,5) SWNT. In the case of DWNTs with nonchiral commensurate walls, the static friction force F_f is significant. The dependence of the friction force on the overlap of the walls, L_{ov}, can be described as $F_f = AL_{\text{ov}} \cos(2\pi L_{\text{ov}}/\delta_z)$, where the period $\delta_z = l_{\text{uc}}/2$ and $A = 0.01$ N/m, see Refs. [45–47]. Analysis of the balance of forces in the memory cell based on a (5,5)@(10,10) DWNT shows that for the overlap greater than the critical

value $l_{cr} = 4$ nm, the sum of the friction force and the Van der Waals force between the source and drain electrodes is always greater than the capillary force. If $L_{ov} > l_{cr}$, the memory cell can be bi-stable in the absence of applied voltage. However, for the nonvolatile cell this condition is adequate only at zero temperature. At nonzero temperatures, the thermal diffusion of the inner wall of the source electrode may overcome the potential barrier, ΔU, between the states 1 and 0. The probability of this to happen is determined by the Arrhenius formula

$$p = \Omega \exp\left(-\frac{\Delta U}{kT}\right), \quad (1)$$

where Ω is the frequency multiplier. DFT and semiempirical calculations of the interaction between the electrodes have been performed to obtain the barrier ΔU as a function of the overlap L_{ov} for the (5,5)@(10,10) DWNT. Previous molecular dynamics (MD) simulations[48, 49] of the $C_{60}@C_{240}$ nanoparticle showed that for temperatures considerably less than the melting temperature of graphite, thermal deformations of the shells did not affect the barrier to their relative reorientations. The barriers obtained by fitting the results of the MD simulations at temperatures between 100 K and 240 K have similar values to those obtained from static calculations at zero temperature.[48, 49] This allows us to estimate the value for the barrier between the logical states 1 and 0 in memory cells based on telescoping DWNTs using static calculations. For reorientation of the shells of the $C_{60}@C_{240}$ nanoparticle, the frequency multiplier Ω was estimated having the value of 650 ± 350 GHz.[48, 49] We expand the semiempirical surface of the intershell interaction energy near the minimum and calculate the frequencies of small relative librations of the shells. The libration frequency averaged over all directions of libration has the value of $\nu = 54$ GHz, an order of magnitude less than that of the frequency multiplier Ω. In our estimations we assume that the ratio Ω/ν remains approximately 10 for different nested carbon nanoobjects including DWNTs.

For the considered memory cell in the state 1, the dependence of the lifetime, $t_L = p^{-1}$, on the overlap of the walls is shown in Figure 2(A). The barrier to the relative motion of nonchiral commensurate walls of DWNT, and hence the barrier between the states 1 and 0, increases with an increase in the radius of DWNT. For the interwall distances close to the experimental value of 3.4 Å, the barrier is also greater for DWNTs with both zigzag walls than for DWNTs with both armchair walls.[46, 47] Thus, Figure 2(A) shows that if the source electrode is made of a DWNT with nonchiral commensurate walls, the longitudinal dimension of the nonvolatile memory cell with both electrodes made of carbon nanotubes can be within one hundred nanometers.

The switching voltage between the logical states 1 and 0 was calculated for the volatile cell with the gate electrode

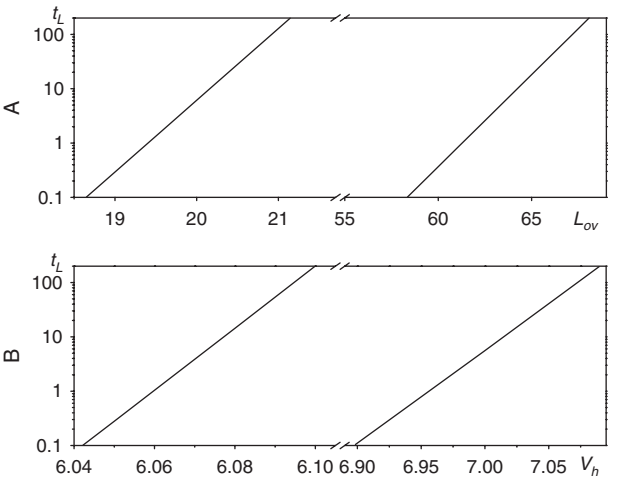

Fig. 2. For the *all carbon* memory cell as described in the text, the dependence of the lifetime t_L, in years, in the the logical state 1: (A) on the overlap of the walls L_{ov}, in nm, (B) on the holding voltage V_h applied to the control electrode, in V. Thin and thick lines correspond to the temperatures of 77 K and 300 K, respectively.

made of a carbon nanotube. We estimate the capacitance C between the source and gate electrodes using macroscopical approach. This approach has been used previously for the description of electrostatic forces in nanoelectromechanical memory cells based on cantilevered,[12, 13, 33] suspended[13, 20, 32, 33] and telescoping nanotubes.[14–16] We consider the inner movable wall of the source electrode and the gate electrode as armatures of cylindrical capacitor. The electrostatic force acting on the movable wall can be then estimated as

$$F_e = \frac{dE_e}{dz} = \frac{d}{dz}\frac{CV^2}{2} = \frac{d}{dz}\frac{\pi\epsilon_0 z V^2}{\ln R_c/R_m} = \frac{\pi\epsilon_0 V^2}{\ln R_c/R_m}, \quad (2)$$

where E_e is the electrostatic energy of the capacitor, V is applied voltage, z is the length of the overlap between the moving wall and the gate electrode, ϵ_0 is vacuum permittivity, and R_m and R_c are radii of the moving wall and the gate electrode, respectively. Assuming the friction force is negligible, the minimum switching voltage V_{s0} between the states 0 and 1 of the device is determined by the condition $F_e > F_c$, and the minimum voltage V_{h0} required to hold the memory cell in the state 1 is determined by the condition $F_e + F_a > F_c$. Substituting the values of the forces F_e, F_c and F_a into the above conditions we obtain $V_{s0} = 6$ V and $V_{h0} = 4.8$ V. In these estimations, the source electrode was taken to be a DWNT with the inner (5,5) wall, the drain electrode was represented by a (5,5) SWNT, and the gate electrode was taken to be a SWNT with the radius $R_c = 1.7$ nm. For three-terminal memory cell, the dependence of the energy barrier ΔU and the frequency multiplier Ω on the holding voltage V_h was calculated for the inner wall of the source electrode of 55.4 nm in length. Using the Arrhenius formula (1) the lifetime of the device in the state 1 was estimated. The dependence of the lifetime in the

state 1 on the holding voltage V_h is shown in Figure 2(B). It was found that the holding voltage V_h required for the lifetime of $t_L = 100$ years only slightly exceeds the minimum holding voltage V_{h0}.

The source electrode of all carbon memory cells can be made of a MWNT. The telescoping motion of the walls,[7–9] the two-terminal memory cell based on telescoping nanotube,[11] and nanotube-based nanomotors[50–53] have been all fabricated with MWNTs. This makes MWNTs most likely candidates for the first fabrication of the three-terminal all carbon memory cell. MWNTs have the interwall distance of about 3.4 Å. According to semiempirical calculations[46, 54] the interwall interaction energy is approximately the same for all pairs of neighbouring walls with the interwall distance of 3.4 Å, and it does not depend on the radius of the walls. In this case, the capillary force F_c can be estimated as

$$F_c = \frac{dU_a S}{dL_{\text{ov}}} = \frac{2\pi R_m U_a dL_{\text{ov}}}{dL_{\text{ov}}} = 2\pi R_m U_a \qquad (3)$$

where S is the surface of the overlap between the moving and fixed walls of the source electrode, U_a is the interwall interaction energy per unit area of the overlap surface. For interwall distances close to the experimental value, U_a increases only slightly and tends to a constant value with the increase of the radius R_m.[46] Therefore, the capillary force is proportional to the radius of the moving wall as can be seen from Eq. (3). We use Eqs. (2) and (3) to estimate the dependence of the minimum switching voltage on the radius of the moving wall assuming that the interwall distance between the moving and fixed walls of the source electrode is 3.4 Å, and the gap between the moving wall of the source electrode and the gate electrode $R_c - R_m =$ 1 nm. The dependence of the minimum switching voltage V_{s0} on the radius R_m of the moving wall is presented in Figure 3. Figure 3 shows that increase in the radius of the moving wall does not lead to a considerable increase in the switching voltage.

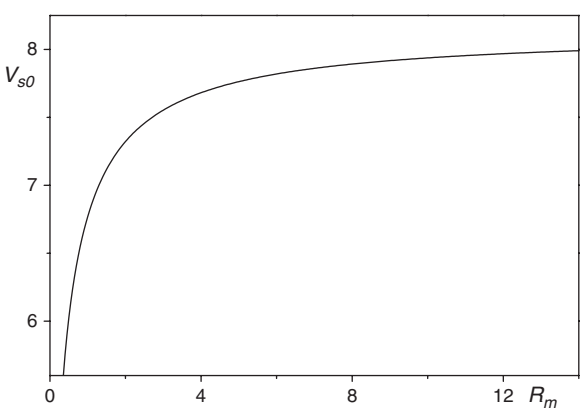

Fig. 3. The dependence of the minimum switching voltage V_{s0} applied to the gate electrode, in V, on the radius R_m of the movable wall of the source electrode, in Å.

The next step in the modelling of all carbon memory cells based on telescoping nanotubes is the simulation of the dynamic behavior. The prime aim of these simulations is to validate the proposed method for avoiding the mechanical and electrical oscillations after the switching between the logical states 0 and 1 in the memory cell. Secondly, we consider the relation between the amplitude of switching voltage pulse and the switching time. Evidently, both these characteristics of the device should have very small values.

The equation of motion for the moving wall of the source electrode is solved numerically taking into consideration electrostatic and capillary forces as well as van der Waals forces of the interaction between the electrodes. All geometrical dimensions of the three-terminal volatile memory cell are taken as described above. Initially, the distance between the moving wall of the source electrode and the drain electrode is taken to be 1nm. The switching time is then calculated for two shapes of the switching voltage pulse having different form of $V(t)$:

Type A

$$V(t) = \begin{cases} V_p, & 0 < t < t_p \\ V_{h0}, & t_p < t < t_s \\ V_h > V_{h0}, & t > t_s \end{cases} \qquad (4)$$

Type B

$$V(t) = \begin{cases} V_p, & 0 < t < t_p \\ 0, & t_p < t < t_s \\ V_h > V_{h0}, & t > t_s \end{cases} \qquad (5)$$

where V_p is the amplitude of the switching voltage pulse which exceeds the minimum switching voltage, i.e., $V_p > V_{s0}$, and V_h is the holding voltage in the state 1.

In both cases, motion of the inner wall of the source electrode towards the drain electrode takes place at the time interval between t_p and t_s with decreasing velocity. Mechanical oscillations of the inner wall can be completely suppressed if, at the moment of time when the holding voltage V_h is applied ($t = t_s$), two conditions are fulfilled: (1) the distance between the inner wall of the source electrode and the drain electrode (z) equals to the distance corresponding to the minimum potential energy of the cell with applied holding voltage (z_m); (2) the inner wall has zero velocity. Evidently, both conditions are fulfilled only if the inner wall has zero velocity at the distance z_m from the drain electrode. As it is shown above the holding voltage only slightly greater than the minimal value V_{h0} is sufficient for continuous stable operation of the memory cell. Therefore, selection of specific values of the holding voltage has negligible effect on the distance z_m and, consequently, on the switching time.

A number of different amplitudes V_p of the switching voltage pulse was considered for both types of the voltage pulse. For any given V_p, the equation of motion for

RESEARCH ARTICLE

the moving wall of the source electrode was solved for different values of the pulse duration, t_p. The pulse duration, t_{p0}, was chosen so that the inner wall acquires zero velocity at the distance z_m from the drain electrode. In this case, time t_s corresponding to the distance z_m, at which the holding voltage V_h should be applied, is the minimum switching time between the logical the states 0 and 1 for a given amplitude V_p of the pulse. The dependence of the pulse duration, t_{p0}, and corresponding switching time, t_s, on the amplitude V_p are shown in Figures 4(A) and (B) for two types of the pulse described by Eqs. (4) and (5). One can expect that the type A of the switching voltage pulse allows using smaller amplitudes of the voltage pulse and therefore might be more suitable for use. However, it was found that the switching time is considerably greater for this type of the pulse. This is due to the following reason. When the minimum holding voltage, V_{h0}, is applied, the dependence of the potential energy of the cell on the position of the moving inner wall of the source electrode exhibits a plateau, and the moving wall is driven towards the drain electrode along this plateau with low velocity for a relatively long time. As a result the switching time is increased. Moreover, it is difficult to choose appropriate pulse duration that gives rise to the fluctuations in the dependence of switching time on the amplitude of the voltage pulse shown in Figure 4(A). As it can be seen from Figure 4, the minimum switching time corresponds to a shorter pulse (type B) where initial rapid increase of velocity of the inner wall followed by the quick decrease takes place. The switching times presented in Figure 4 correspond to the memory cell with overall size less than 100 nm. As the switching time is proportional to $(m)^{-1/2}$, where m is the mass of the wall, the switching time is increased with increase of the cell size. The proposed method of increasing the operational frequency of nanoelectromechanical volatile memory cells allows for a three-terminal all carbon memory cell based on telescoping nanotubes to achieve the frequencies in the range of 100 GHz.

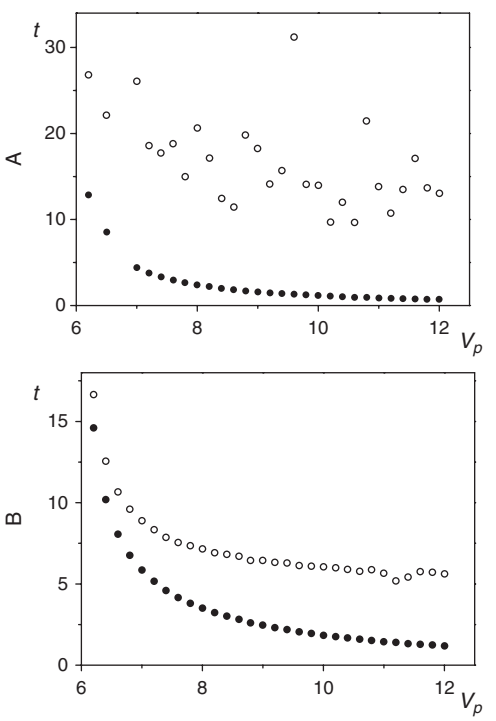

Fig. 4. The dependence of the pulse duration t_{p0}, in ps, (dark circles) and the corresponding switching time t_s, in ps, (light circles) on the amplitude V_p of the switching voltage pulse, in V. Figures A and B correspond to the type A and B of the switching voltage pulse.

3. CONCLUSIVE REMARKS

A new method for increasing the operational frequency of volatile nanoelectromechanical memory cells is proposed. An appropriate choice of the shape of the switching voltage pulse suppresses the oscillations in the memory cell leading to unambiguous determination of the logic state immediately after switching. The proof of the method is demonstrated in the simulations of all carbon three-terminal memory cells based on telescoping motion of the walls of carbon nanotubes. The operational characteristics of all carbon three-terminal memory cells have been also investigated.

It is predicted that for the volatile memory cells the proposed method allows reaching the operational frequencies as high as 100 GHz. It is found that the switching voltage is required to be less than 10 V for any size of the volatile memory cell. The influence of thermodynamic fluctuations on the stability of both nonvolatile and volatile memory cells in the logical state 1 has been studied. It is shown that the nonvolatile cells are stable at room temperature even with linear dimensions of tens nanometers. The stability of the memory cells at room temperature can be achieved and maintained by a slight increase in voltage compared to that required to keep the cell in the the logical state 1 at zero temperature.

Acknowledgments: E. Bichoutskaia gratefully acknowledges financial support of an EPSRC Career Acceleration Fellowship. This work was performed during A. M. Popov short visit to the University of Nottingham funded by the Royal Society. This work was also partially supported by the Russian Foundation of Basic Research (A. M. Popov, Y. E. Lozovik and A. S. Kulish grants 08-02-00685 and 08-02-90049-Bel).

References and Notes

1. T. Rueckes, K. Kim, E. Joselevich, G. Y. Tseng, C. L. Cheung, and C. M. Lieber, *Science* 289, 94 (**2000**).
2. S. W. Lee, D. S. Lee, R. E. Morjan, S. H. Jhang, M. Sveningsson, O. A. Nerushev, Y. W. Park, and E. E. B. Campbell, *Nano Lett.* 4, 2027 (**2004**).

3. S. Axelsson, E. E. B. Campbell, L. M. Jonsson, J. M. Kinaret, S. W. Lee, Y. W. Park, and M. Sveningsson, *New J. Physics* 7, 245 **(2005)**.
4. J. E. Jang, S. N. Cha, Y. J. Choi, D.-J. Kang, T. P. Butler, D. G. Husko, J. E. Jung, J. M. Kim, and G. A. J. Amaratunga, *Appl. Phys. Lett.* 87, 163114 **(2005)**.
5. J. E. Jang, S. N. Cha, Y. J. Choi, G. A. J. Amaratunga, D. J. Kang, D. G. Husko, J. E. Jung, and J. M. Kim, *Nat. Nanotechnol.* 3, 26 **(2008)**.
6. E. Dujardin, V. Derycke, M. F. Goffman, R. Lefevre, and J. P. Bourgoin, *Appl. Phys. Lett.* 87, 193107 **(2005)**.
7. M. F. Yu, O. Lourie, M. J. Dyer, K. Moloni, and R. S. Ruoff, *Science* 287, 637 **(2004)**.
8. J. Cumings and A. Zettl, *Science* 289, 602 **(2000)**.
9. A. Kis, K. Yensen, S. Aloni. W. Mickelson, and A. Zettl, *Phys. Rev. Lett.* 97, 025501 **(2006)**.
10. L. Forro, *Science* 289, 5479 **(2000)**.
11. V. V. Deshpande, H. Y. Chiu, H. W. C. Postma, C. Miko, L. Forro, and M. Bockrath, *Nano Lett.* 6, 1092 **(2006)**.
12. K. V. Bulashevic and S. V. Rotkin, *JETP Letters* 75, 205 **(2002)**.
13. M. Dequesnes, S. V. Rotkin, and N. R. Aluru, *Nanotechnology* 13, 120 **(2002)**.
14. L. Maslov, *Nanotechnology* 17, 2775 **(2006)**.
15. A. M. Popov, E. Bichoutskaia, Yu. E. Lozovik, and A. S. Kulish, *Phys. Stat. Sol. A* 204, 1911 **(2007)**.
16. J. W. Kang and Q. Jiang, *Nanotechnology*, 18, 095705 **(2007)**.
17. E. Bichoutskaia, A. M. Popov, and Y. E. Lozovik, *Mater. Today* 11, 38 **(2008)**.
18. L. M. Jonsson, T. Nord, and J. M. Kinaret, *J. Appl. Phys.* 96, 629 **(2004)**.
19. S. Xiao, D. R. Andersen, and W. Yang, *Nanoscale Res. Lett.* 3, 416 **(2008)**.
20. J. W. Kang, O. K. Kwon, J. H. Lee, H. J. Lee, Y.-J. Song, Y.-S. Yoon, and H. J. Hwang, *Physica E* 33, 41 **(2006)**.
21. I. V. Lebedeva, A. A. Knizhnik, A. M. Popov, Yu. E. Lozovik, and B. V. Potapkin, *Nanotechnology* 20, 105202 **(2009)**.
22. R. P. Gao, Z. L. Wang, Z. G. Bai, W. A. de Heer, L. M. Dai, and M. Gao M, *Phys. Rev. Lett.* 85, 622 **(2000)**.
23. V. Sazonova, Y. Yaish, H. Ustunel, D. Roundy, T. A. Arias, and P. L. McEuen, *Nature* 431, 284 **(2004)**.
24. K. Jensen, G. Girit, W. Mickelson, and A. Zettl, *Phys. Rev. Lett.* 96, 215503 **(2006)**.
25. P. Poncharal, Z. L. Wang, D. Ugarte, and W. A. de Heer, *Science*. 283, 1513 **(1999)**.
26. B. Reulet, A. Y. Kasumov, M. Kociak, R. Deblock, I. I. Khodos, Y. B. Gorbatov, V. T. Volkov, C. Journet, and H. Bouchiat, *Phys. Rev. Lett.* 85, 2829 **(2000)**.
27. S. T. Purcell, P. Vincent, C. Journet, and V. T. Binh, *Phys. Rev. Lett.* 89, 276103 **(2002)**.
28. H. Jiang, M.-F. Yu, B. Liu, and Y. Huang, *Phys. Rev. Lett.* 93, 185501 **(2004)**.
29. C.-C. Ma, Y. Zhao, Y.-C. Yam, G. Chen, and Q. Jiang, *Nanotechnology* 16, 1253 **(2005)**.
30. J. M. Kinaret, T. Nord, and S. Viefers, *Appl. Phys. Lett.* 82, 1287 **(2003)**.
31. H. J. Hwang and J. W. Kang, *Physica E* 27, 163 **(2005)**.
32. M. Dequesnes, Z. Tang, and N. R. Aluru, *J. Eng. Mater. Technol.* 126, 130 **(2004)**.
33. C. Ke, H. D. Espinosa, and N. Pungo, *J. Appl. Mech.* 72, 726 **(2005)**.
34. Z. Shen, S. Lie, Z. Xue, and X. Gu, *Int. Journ. of Nanoscience* 1, 575 **(2002)**.
35. S. C. Tsang, P. J. F. Harris, and M. L. H. Creen, *Nature* 362, 520 **(1993)**.
36. P. M. Ajayan, T. W. Ebbesen, T. Ichihashi, S. Iijima, K. Tanigaki, and H. Huira, *Nature* 362, 522 **(1993)**.
37. K. El-Hami and K. Mitsushige, *Int. Journ. of Nanoscience* 2, 125 **(2003)**.
38. K. Hirahara, M. Kociak, S. Bandow, T. Nakahira, K. Iton, Y. Saito, and S. Iijima, *Phys. Rev. B* 73, 195420 **(2006)**.
39. M. C. Hersam, *Nat. Nanotechnol.* 3, 387 **(2008)**.
40. P. R. Briddon and R. Jones, *Phys. Stat. Sol.* 217, 131 **(2000)**.
41. G. B. Bachelet, D. R. Hamann, and M. Schlüter, *Phys. Rev. B* 26, 4199 **(1982)**.
42. J. P. Perdew and Y. Wang, *Phys. Rev. B* 45, 13244 **(1992)**.
43. J. Kong, C. A. White, A. I. Krylov, C. D. Sherrill, R. D. Adamson, T. R. Furlani, M. S. Lee, A. M. Lee, S. R. Gwaltney, T. R. Adams, C. Ochsenfeld, A. T. B. Gilbert, G. S. Kedziora, V. A. Rassolov, D. R. Maurice, N. Nair, Y. Shao, N. A. Besley, P. E. Maslen, J. P. Dombroski, H. Daschel, W. Zhang, P. P. Korambath, J. Baker, E. F. C. Byrd, T. Van Voorhis, M. Oumi, S. Hirata, C.-P. Hsu, N. Ishikawa, J. Florian, A. Warshel, B. G. Johnson, P. M. W. Gill, M. Head-Gordon, and J. A. Pople, *J. Comput. Chem.* 21, 1532 **(2000)**.
44. L. A. Girifalco, M. Hodak, and R. S. Lee, *Phys. Rev. B* 62, 13104 **(2000)**.
45. E. Bichoutskaia, A. M. Popov, A. El-Barbary, M. I. Heggie, and Yu. E. Lozovik, *Phys. Rev. B* 71, 113403 **(2005)**.
46. A. V. Belikov, Yu. E. Lozovik, A. G. Nikolaev, and A. M. Popov, *Chem. Phys. Lett.* 385, 72 **(2004)**.
47. E. Bichoutskaia, A. M. Popov, M. I. Heggie, and Yu. E. Lozovik, *Phys. Rev. B* 73, 045435 **(2006)**.
48. Yu. E. Lozovik and A. M. Popov, *Chem. Phys. Lett.* 328, 355 **(2000)**.
49. Yu. E. Lozovik and A. M. Popov, *Physics of the Solid State* 186, 44 **(2002)**.
50. A. M. Fennimore, T. D. Yuzvinsky, W. Q. Han, M. S. Fuhrer, J. Cumings, and A. Zettl, *Nature* 424, 408 **(2003)**.
51. B. Bourlon, D. C. Glatti, L. Forro, and A. Bachtold, *Nano Lett.* 4, 709 **(2004)**.
52. A. Barreiro, R. Rurali, E. R. Hernandez, J. Moser, T. Pichler, L. Forro, and A. Bachtold, *Science* 320, 775 **(2008)**.
53. A. Subramanian, L. X. Dong, J. Tharian, U. Sennhauser, and B. J. Nelson, *Nanotechnology* 18, 075703 **(2007)**.
54. R. Saito, R. Matsuo, T. Kimura, G. Dresselhaus, and M. S. Dresselhaus, *Chem. Phys. Lett.* 348, 187 **(2001)**.

Received: 22 July 2009. Accepted: 30 October 2009.